Mixing characteristics of refractory black carbon aerosols determined by a tandem CPMA-SP2 system at an urban site in Beijing

Supplementary

5   **Table S1. Abbreviations and symbols used in this paper**

Abbreviation/symbols	Full name/explanation
SP2	Single particle soot photometer (DMT Technologies)
DMA	Differential mobility analyzer (TSI Inc.)
CPMA	Couette centrifugal particle mass analyzer (Cambustion, Ltd.)
CPC	Condensation particle counter (TSI Inc.)
rBC	Refractory black carbon determined by SP2 through laser-induced incandescence method
MED	Mass equivalent diameter
MMD	Mass median diameter
D_p & D_c	Diameter of rBC-containing particles and rBC
LEO	Leading-edge-only fitting method
M_p & M_{coat} & M_{rBC}	Mass of rBC-containing particles, mass of coating material, mass of rBC
M_R	M_{coat}/M_{rBC}
D_{mob}	Mobility diameter determined by DMA
ρ_{eff}	Effective density
n_{coat} & n_{rBC}	Refractive index of coating material and rBC
D_{fm}	Mass fractal dimension
E_{abs}	Absorption enhancement of rBC-containing particles compared to bare rBC
SCS_{sp2}	Scattering cross section of rBC-containing particles measured by SP2
SCS_{mie}	Scattering cross section of rBC-containing particles calculated using the Mie theory
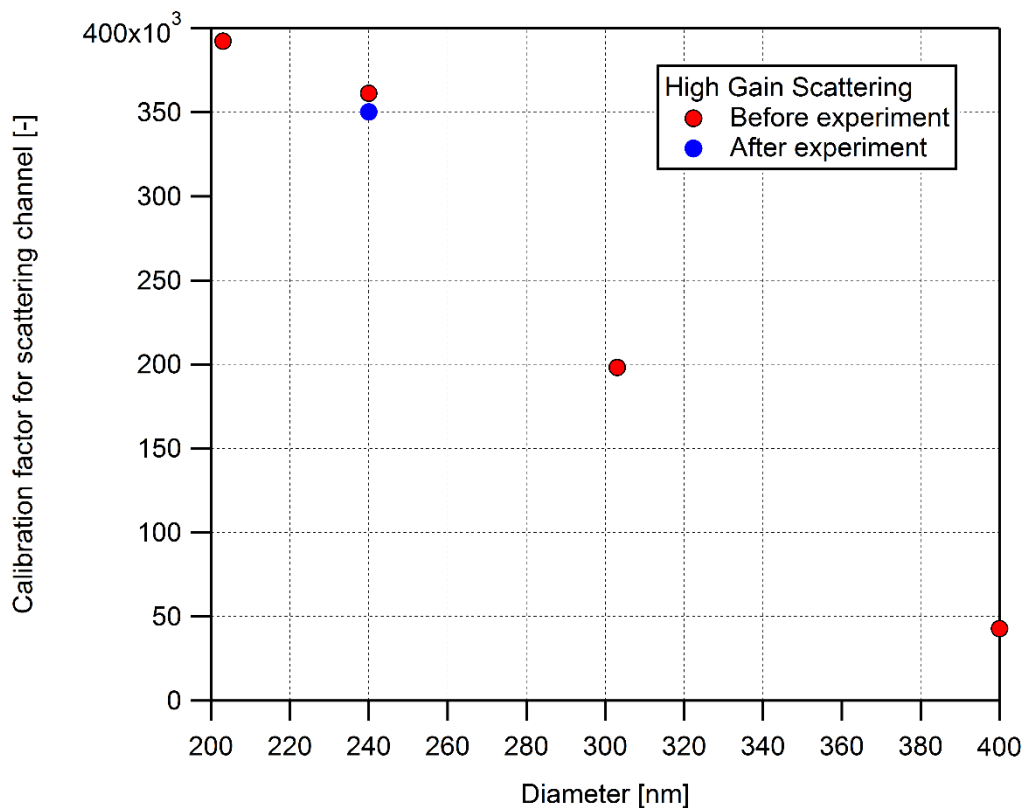
Figure S1 PSL calibration for high gain scattering channel before and after the investigation. (For 240 nm PSL, the calibration factor is approximately the same before and after the campaign, demonstrating the stable condition for SP2).
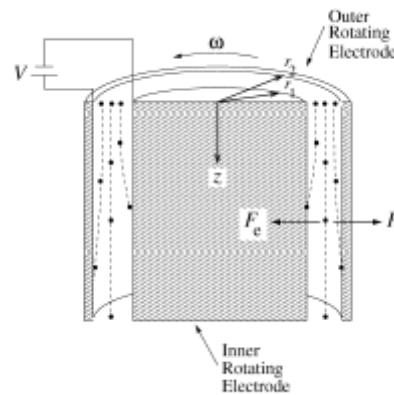
Figure S2 Schematic diagram of CPMA.
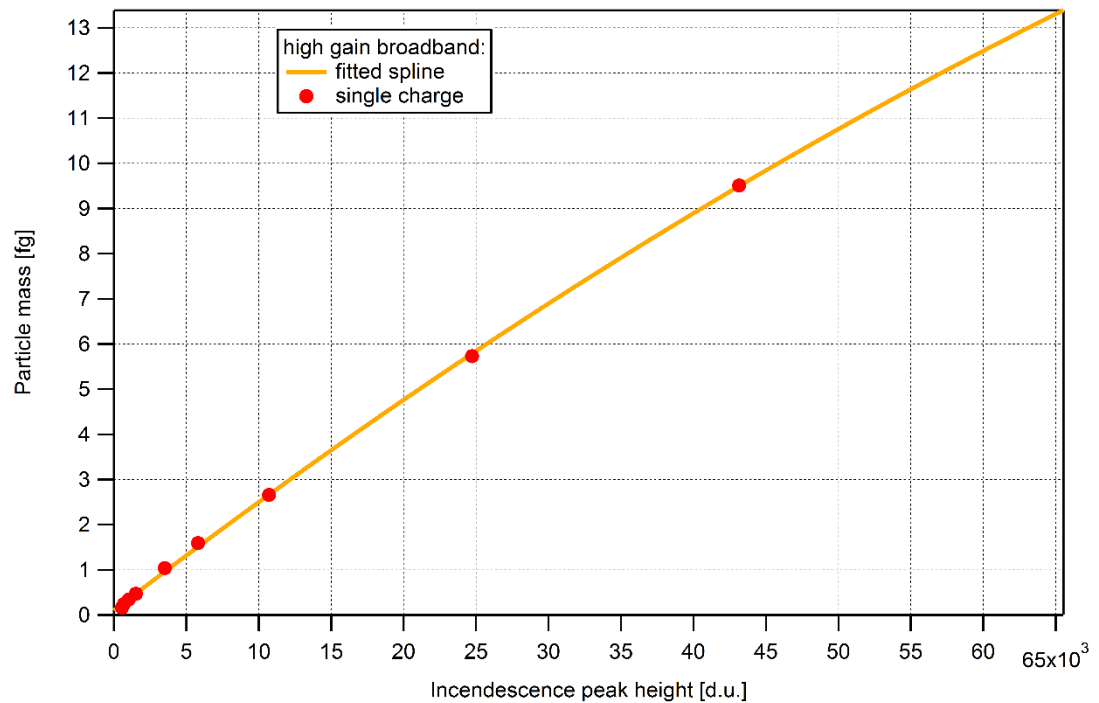
Figure S3 Calibration curve for broadband high gain channel (CPMA+SP2).

20
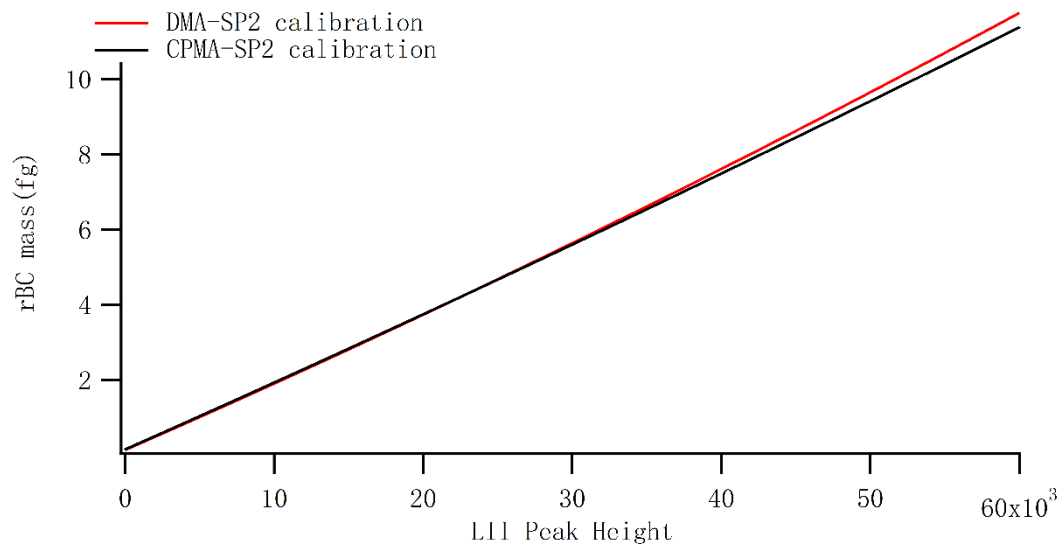
Figure S4 Comparison between CPMA-SP2 calibration factor and DMA-SP2 calibration factor.
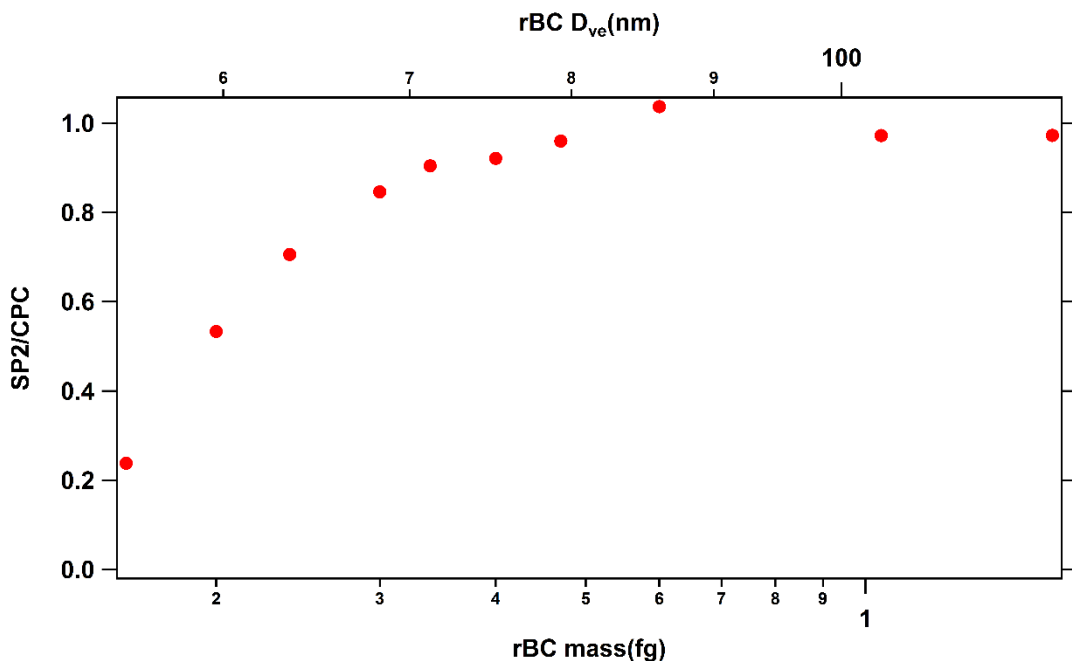
Figure S5 SP2's detection efficiency of Aquadag for a laser current of 1750 mA.

Sensitivity of refractive index and density to Mie-calculation

The estimation of the mixing state of rBC-containing particles was highly dependent on the parameters in the Mie scattering calculations. As shown in Table S3, previous studies adopted different parameters for the Mie calculation (Liu et al., 2014;Moteki et al., 2012;Shiraiwa et al., 2008), considering the different chemo-physical properties of rBC-containing particles in various environments. In the present study, a sensitivity test was conducted to calculate the RCT (Dp/Dc) under the assumption of different sets of parameters. The rBC-containing particles with $Dc=180\pm10$ nm on June 2 were selected to perform the sensitivity test. In previous studies, the refractive indices of the coatings of rBC-containing particles in a Mie-calculation were similar, ranging from 1.45-0i to 1.50-0i, and the rBC material density ranged from 1.77 to 2.0 g/cm^3. However, the calculated refractive indices of the rBC core are much different, ranging from 1.76-0.44i to 2.26-1.26i. The lower and upper bounds of the variation range were used in the sensitivity test. The parameters ($n_{rBC}=2.26-1.26i$, $n_{coat}=1.48$, $\rho_{rBC}=1.8$ g/cm^3) were regarded as the control group. The sensitivity experiments were performed by changing one parameter and not changing the other two parameters to calculate the RCT. As shown in Figure S8, a higher n_{coat} increases the scattering efficiency of coating, leading to a reduction in the deductive D_p and RCT. A larger assumed ρ_{rBC} results in a decrease in D_c as D_c is inferred from M_{rBC}. According to the Mie calculation, rBC with a

smaller D_c core scatters less light and more scattering is attributed to coating, leading to an increase of D_p. Thus, RCT tends to increase due to the higher D_p and lower D_c when using a lager ρ_{rBC}. However, the effect of ρ_{rBC} and n_{coat} on RCT is relatively small compared to the effect of n_{rBC}. The mode of RCT significantly changes from 1 to 1.3 under different assumptions of n_{rBC}. A larger n_{rBC} increases the scattering efficiency of the rBC core and less scattering is attributed to coating, leading to less inverting of D_p and RCT. This result is similar to (Taylor et al., 2015) in that the uncertainty in the Mie calculation caused by the refractive index of the rBC core is much larger than the coating refractive index and rBC material density.

Table S2. Different parameters from previous studies

n_{rBC}	n_{coat}	ρ_{rBC} (g/cm^3)	References
2.26-1.26i	1.48+0i	1.8	(Liu et al., 2014)
1.95-0.79i	1.48+0i	1.9	(Subramanian et al., 2010)
1.76-0.44i	1.52+0.015i	2	(Moteki et al., 2012)
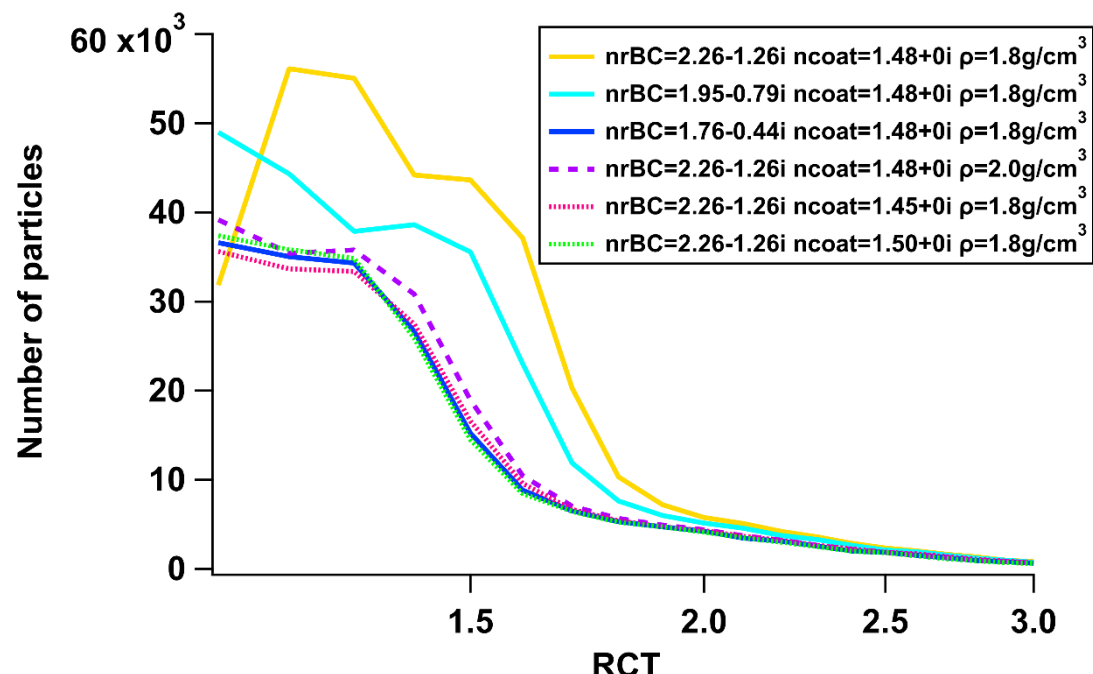
Figure S6. RCT derived from the Mie calculation under different assumptions of parameters at Dc=180±10 nm.

When RCT is higher than 2.5, the RCT distributions derived from different n_{rBC} tend to overlap, whereas the RCT distribution varies markedly when the RCT is much lower. Thus, the sensitivity of Mie-

calculation parameters to the RCT within different RCT ranges was evaluated as illustrated in Table 4. The RCT is first calculated using the parameters in the control group to classify rBC-containing particles into different RCT ranges, then the Mie calculation was repeatedly performed using varied parameters on particles in different RCT ranges. The sensitivity of RCT to Mie-calculation parameters presents notable dependence on RCT ranges. When the RCT is in the range of 1–1.5, using n_{rBC}=1.76-0.44i will result in a 21.6% overestimate of the average RCT compared to the average RCT derived from the control group. Such an overestimate significantly decreases to 0.5% in a RCT range of 3.5–4. A similar trend is found in the ρ_{rBC} sensitivity test, where the overestimate of RCT by using ρ_{rBC} =2 g/cm^3 also decreases with an increase in the RCT range. However, an opposite tendency appears in terms of n_{coat}, in which the overestimate or underestimate of RCT exhibits a positive correlation with the RCT range. In smaller RCT ranges, the rBC core occupies a larger fraction of the rBC-containing particles; thus, the Mie calculation is more sensitive to the parameters related to the rBC core, i.e., n_{rBC} and ρ_{rBC}. However, with an increase in the RCT range, the rBC fraction decreases and the coating fraction increases, leading to greater dependence of the Mie calculation on parameters related to coatings, i.e., n_{coat}.

Determination of parameters

In this study, a DMA+SP2 system was adopted to determine the optimal refractive indices. Ambient particles of known mobility sizes (200 nm, 250 nm, 300 nm) were selectively inserted into the SP2. We selected different refractive indices to calculate the optical size of ambient purely scattering particles, and the best agreement between the estimated optical size and mobility size selected by DMA was achieved when n_{coat}=1.48-0i. This is consistent with the values (1.5–0i) reported in previous studies (Laborde et al., 2013;Gong et al., 2016). The difference is primarily caused by the different composition of purely scattering particles, as the refractive indices varies with composition (1.51 for $(NH4)_2SO_4$, 1.53 for Nacl, 1.44–1.5 for secondary organic aerosol) (Toon et al., 1976;Schnaiter et al., 2003;Nakayama et al., 2010).

(Moteki et al., 2010;Taylor et al., 2015) demonstrated that n_{rBC}=2.26-1.26i is most suitable for the urban rBC that is primarily emitted by vehicles, whereas (Liu et al., 2014) hypothesized that n_{rBC}=2.26-1.26i may not be suitable for rBC emitted from solid fuel. In terms of size distribution and fractal dimension, rBC was primarily emitted by on-road vehicles, indicating the selected n_{rBC}=2.26-1.26i was appropriate during the summer in Beijing. The selection of n_{rBC} is important as most of the RCT is in the range of 1–

90 2, as shown in Figure S8, which implies RCT is very sensitive to n_{rBC}. During winter, rBC is likely to be emitted from various sources; therefore, the selection of n_{rBC} seems is complicated. However, rBC tends to be more thickly coated during winter, suggesting RCT is less sensitive to n_{rBC} during winter. For simplicity, the same $n_{rBC}=2.26-1.26i$ value can be used in both winter and summer. However, RCT is more sensitive to n_{coat} when rBC is thickly coated. (Gong et al., 2016) reported an extremely high RCT

95 (~2–8) during winter in Shanghai. The selection of n_{coat} is vital in such extremely polluted cases.

Table S3. Average RCT within different RCT ranges under varied Mie-calculation parameters. (The RCT is first calculated using standard parameters to classify particles into different RCT ranges. Then, the Mie calculation is repeatedly performed using varied parameters on particles in different RCT ranges. The
100 **percentages in the brackets denote the change rate of the average RCT compared to the average RCT calculated using the standard parameters).**

	RCT range (derived from $n_{rBC}=2.26-1.26i$, $n_{coat}=1.48$, $\rho_{rBC}=1.8$ g/cm3)					
	1–1.5	1.5–2	2–2.5	2.5–3	3–3.5	3.5–4
RCT avg. (Control)	1.14	1.69	2.21	2.71	3.21	3.69
RCT avg. $n_{rBC}=1.95-0.79i$ (Experiments)	1.28 (+11.9%)	1.82 (+8%)	2.31 (+4.5%)	2.78 (+2.7%)	3.25 (+1.3%)	3.70 (+0.5%)
RCT avg. $n_{rBC}=1.76-0.44i$	1.39 (+21.6%)	1.88 (+11.5%)	2.35 (+6.0%)	2.79 (+3.3%)	3.26 (+1.4%)	3.70 (+0.5%)
RCT avg. $n_{coat}=1.45$	1.15 (+0.5%)	1.71 (+1.5%)	2.26 (+2.0%)	2.77 (+2.3%)	3.30 (+2.5%)	3.78 (+2.6%)
RCT avg. $n_{coat}=1.5$	1.14 (-0.3%)	1.67 (-0.9%)	2.19 (-1.2%)	2.67 (-1.4%)	3.16 (-1.6%)	3.63 (-1.7%)
RCT avg. $\rho_{rBC}=2$ g/cm^3	1.17 (+2.1%)	1.70 (+1.6%)	2.21 (+0.8%)	2.72 (+0.4%)	3.22 (+0.1%)	3.69 (0%)

105

110

Figure S7 Relationship between effective density and mobility diameter of Aquadag measured in the present study and in previous studies.
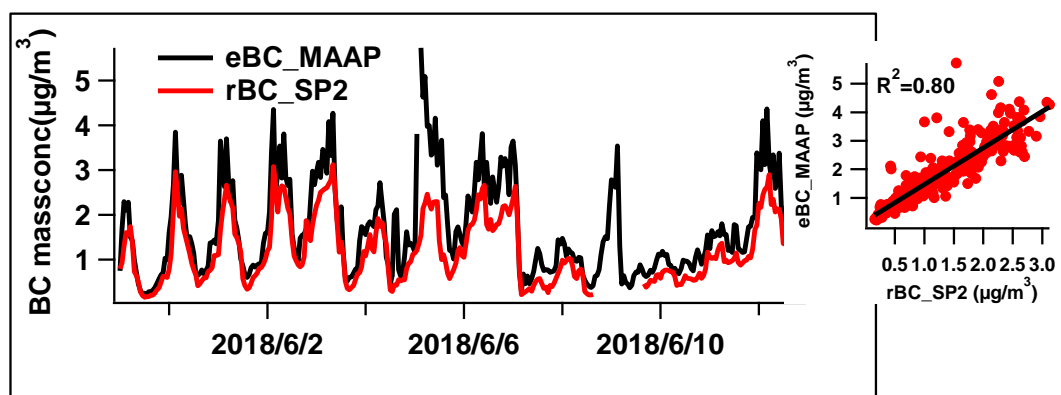
115 **Figure S8 Comparison of the mass concentration of BC measured using MAAP and SP2.**
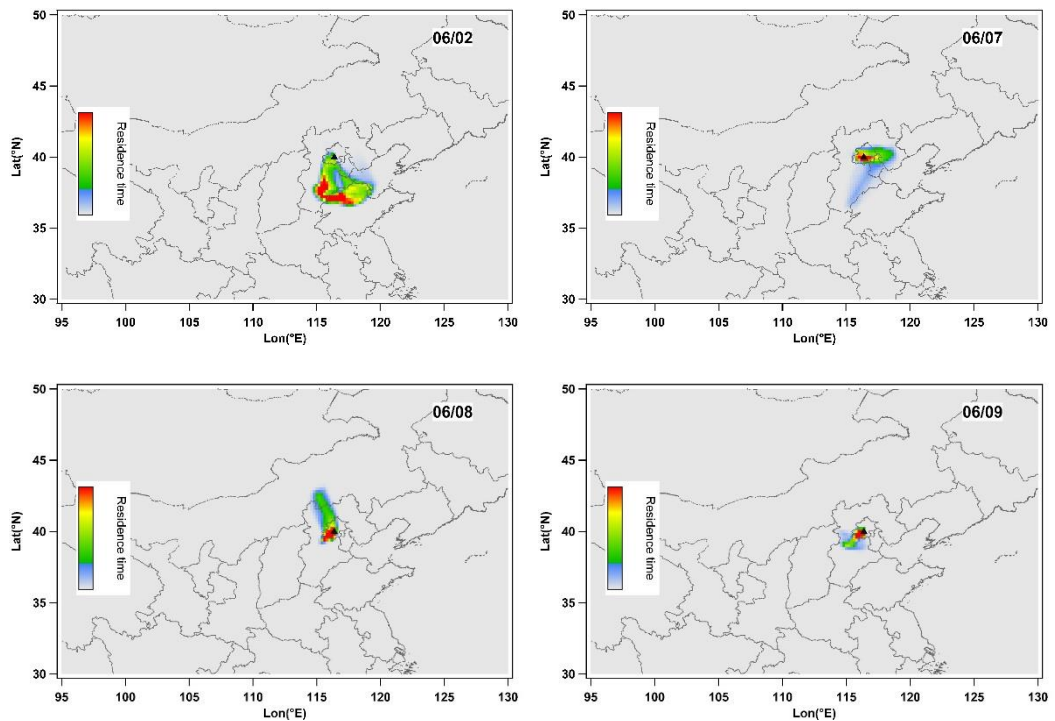
120   **Figure S9 One-day footprints on June 2, 7, 8 and 9 calculated using the FLEXPART dispersion model.**
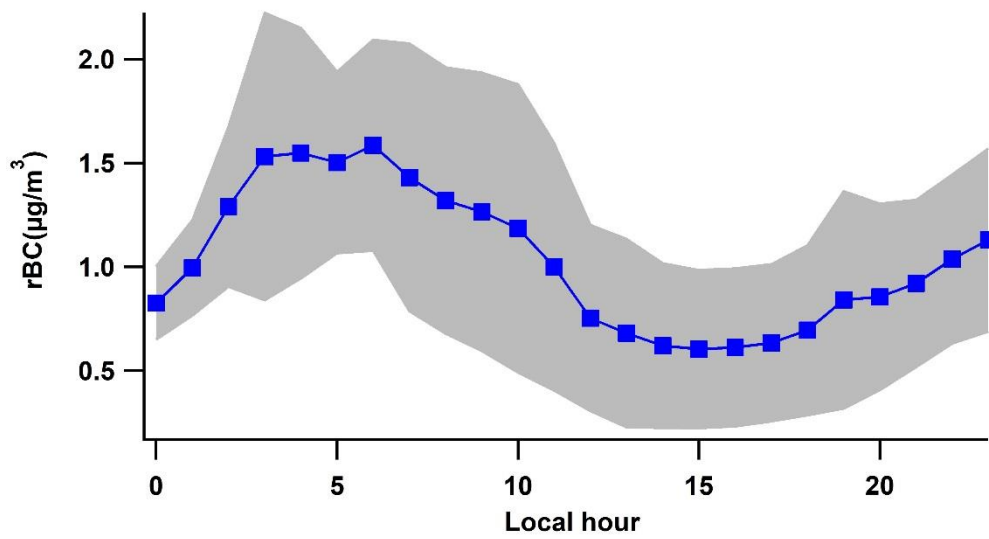
Figure S10 Diurnal variation of rBC mass concentration during the observation period.

125
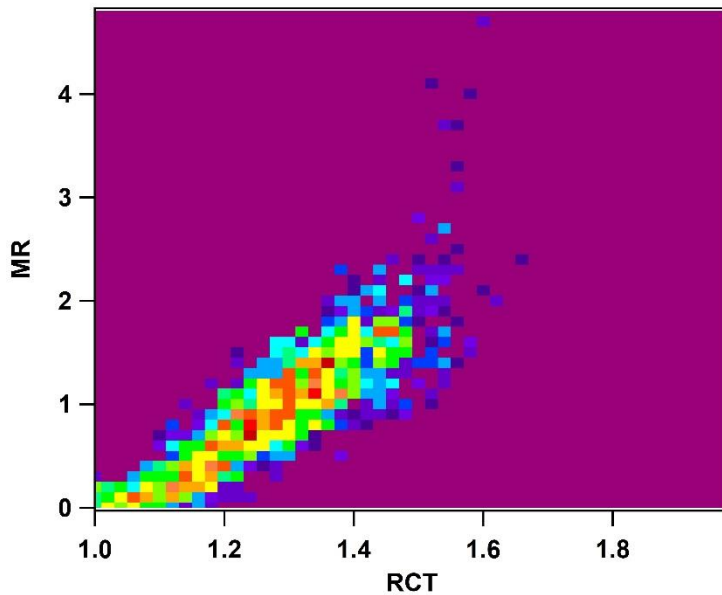
Figure S11 Dependence of the mass ratio (MR = M$_{coat}$/M$_{rBC}$) between the coating material (M$_{coat}$) and rBC

core (M$_{rBC}$) as a function of RCT(Dp/Dc). Colors in the plot represent the number of particles in each bin.

130
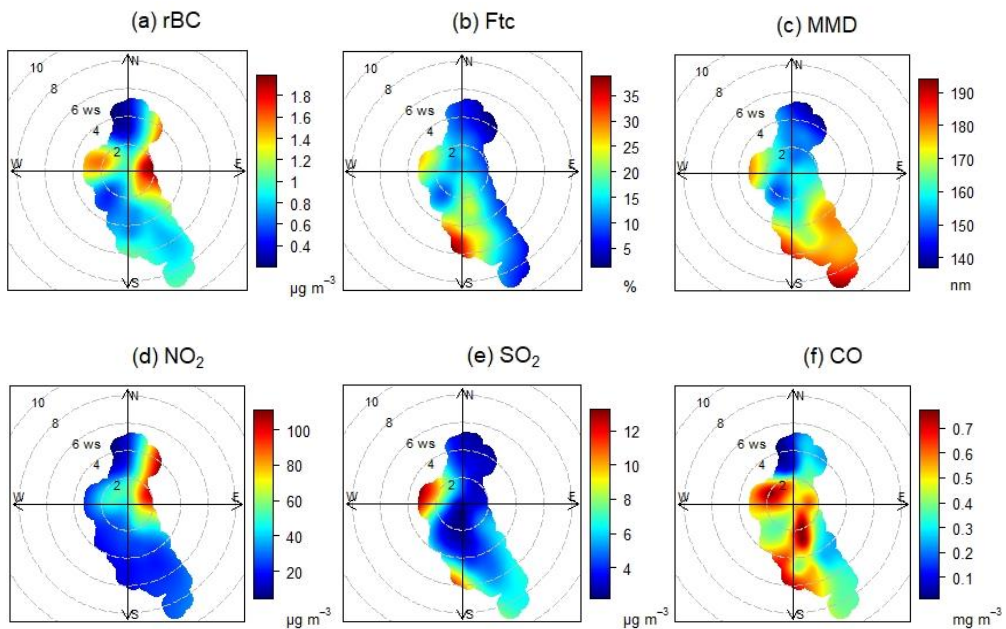
Figure S12 Dependence of rBC properties ((a) mass concentration, (b) Ftc, (c) MMD) and mass

concentration ((d) NO2, (e) SO2, (c) CO) on wind speed and wind direction during the investigation.

135